

**SELF-ASSEMBLED FILMS AS CORROSION PROTECTIVE  
COATINGS FOR METAL SURFACES**

by

Gary N. Robinson, Qing Dai, Paul L. Kebabian, and Andrew Freedman

Final Report

U.S. Army Research Office

Contract No. DAAH04-95-C-0012

Aerodyne Research, Inc.  
45 Manning Road  
Billerica, MA 01821-3976

Phone: (978) 663 9500

Fax: (978) 663 4918

# REPORT DOCUMENTATION PAGE

Form Approved  
OMB NO. 0704-0188

Public reporting burden for this collection of information is estimated to average 1 hour per response, including the time for reviewing instructions, searching existing data sources, gathering and maintaining the data needed, and completing and reviewing the collection of information. Send comment regarding this burden estimate or any other aspect of this collection of information, including suggestions for reducing this burden, to Washington Headquarters Services, Directorate for Information Operations and Reports, 1215 Jefferson Davis Highway, Suite 1204, Arlington, VA 22202-4302, and to the Office of Management and Budget, Paperwork Reduction Project (0704-0188), Washington, DC 20503.

1. AGENCY USE ONLY (Leave blank)		2. REPORT DATE 3-31-97		3. REPORT TYPE AND DATES COVERED Final 3/15/95 - 12/31/96	
4. TITLE AND SUBTITLE Self-Assembled Films as Corrosion Protective Coatings for Metal Surfaces				5. FUNDING NUMBERS DAAH04-95-C-0012	
6. AUTHOR(S) Robinson, G.N., Dai, Q., Kebabian, P.L., and Freedman, A.					
7. PERFORMING ORGANIZATION NAME(S) AND ADDRESS(ES) Aerodyne Research, Inc. 45 Manning Road Billerica, MA 01821				8. PERFORMING ORGANIZATION REPORT NUMBER	
9. SPONSORING / MONITORING AGENCY NAME(S) AND ADDRESS(ES) U.S. Army Research Office P.O. Box 12211 Research Triangle Park, NC 27709-2211				10. SPONSORING / MONITORING AGENCY REPORT NUMBER ARO 33609.4-CH-ERI	
11. SUPPLEMENTARY NOTES The views, opinions and/or findings contained in this report are those of the author(s) and should not be construed as an official Department of the Army position, policy or decision, unless so designated by other documentation.					
12a. DISTRIBUTION / AVAILABILITY STATEMENT  Approved for public release; distribution unlimited.				12 b. DISTRIBUTION CODE	
13. ABSTRACT (Maximum 200 words)  In this Final Report, we describe research performed on the corrosion inhibitive properties of self-assembled monolayers (SAMs) of stearic acid and 10,12-pentacosadiynoic acid (10,12-PDA) on aluminum. Infrared (IR) and X-ray photoelectron spectroscopy, in addition to wetting measurements, were employed to study the corrosion process. Monolayers of stearic acid on aluminum surfaces were found to profoundly affect the wettability of Al surfaces by concentrated sulfuric acid, but not to act as a significant barrier to corrosion. However, to the extent that the SAM coating limits the wettability of the metal surface, it reduces the degree of corrosion. Toward our goal of creating impermeable organic layers, we studied the adsorption and subsequent UV-induced cross linking of 10,12-PDA acid on aluminum. IR and XPS studies as well as macroscopic wettability and corrosion experiments indicate that the resulting coverage of 10,12-PDA on the aluminum surface is very low. We propose experiments which will focus on improving PDA adsorption on Al and on the effect of UV-induced cross linking on the corrosion resistance.					
14. SUBJECT TERMS				15. NUMBER OF PAGES	
				16. PRICE CODE	
17. SECURITY CLASSIFICATION OR REPORT UNCLASSIFIED		18. SECURITY CLASSIFICATION OF THIS PAGE UNCLASSIFIED		19. SECURITY CLASSIFICATION OF ABSTRACT UNCLASSIFIED	
				20. LIMITATION OF ABSTRACT  UL	

## SCIENTIFIC PROGRESS AND ACCOMPLISHMENTS

The goal of the our research program was to investigate the potential use of self-assembled films of organic molecules as corrosion protective primer coatings for metal surfaces. Monolayer and multilayer films are deposited on metal surfaces by immersing the substrate in solutions containing suitably functionalized organic compounds. The molecules spontaneously chemisorb on the metal surface to form ordered, densely packed, and highly impermeable layers. The primary advantage of these films over currently used heavy metal-based primer materials is that they are both non-hazardous to the environment and non-toxic.

Our research focused on two broad issues: (1) development and refinement of diagnostic techniques for measuring the atmospheric corrosion of metal substrates, and (2) deposition of self-assembled monolayers (SAMs) on aluminum surfaces and assessing the corrosion inhibitive properties of these monolayers.

In the first category, we have completed a study of sulfuric acid-induced corrosion of aluminum using Fourier transform infrared reflection absorption spectroscopy (FT-IRAS) to identify and quantify corrosion products. (The results of this study are reported in an article published in *J. Electrochem. Soc.* **142**, 4063-4069 (1995).) Sulfuric acid is the principal corrosive agent in polluted urban and industrial atmospheres. Sub-micron thick films of sulfuric acid were formed on aluminum surfaces in vacuum by co-depositing  $\text{SO}_3$  and  $\text{H}_2\text{O}$ . Changes in the chemical composition of the sulfuric acid layer (including the appearance of sulfate ions and hydrated aluminum ions) resulting from corrosion of the aluminum substrate, were monitored as a function of reagent concentration and relative humidity. The rate of corrosion was enhanced by both higher relative humidities and increased rates of sulfuric acid deposition.

Also in this category, we have completed an investigation of the morphological changes that occur on an aluminum surface undergoing corrosion by submicron-sized sulfuric acid droplets. In this study (conducted in collaboration with Miquel Salmeron at Lawrence Berkeley Laboratory), we employed Scanning Polarization Force Microscopy to image the size changes that occur in concentrated sulfuric acid droplets as the relative humidity is varied. We also were able to observe the onset of aluminum corrosion and the formation of aluminum sulfate salts as products of the corrosion process. These results have been published in *J. Phys. Chem.* **100**, 9-11 (1996). (Please note that the support of the Army was inadvertently omitted from the

acknowledgent section of this paper. We greatly regret this oversight.)

Our research on the use of ultrathin organic films as corrosion protective coatings for metal surfaces has focused initially on deposition of SAMs of stearic acid ( $\text{CH}_3(\text{CH}_2)_{16}\text{COOH}$ ) on aluminum surfaces. Alkanoic acids are known to chemisorb on the native oxide present on aluminum surfaces that have been exposed to air. The monolayers were formed in the following manner. 2000 Å of aluminum were vapor deposited on polished 4 in. diameter silicon wafers. The vapor deposition chamber was vented to pure oxygen so that the native oxide layer on the aluminum surface would not contain impurities from ambient room air. Immediately after removing the metal coated wafers from the vacuum chamber they were immersed in a 1mM solution of stearic acid in HPLC grade hexadecane. The hexadecane was eluted through an activity 1 alumina column prior to making the solution in order to remove impurities. The wafers were allowed to remain immersed in the solution for ~24 hrs whereupon they were removed and rinsed, alternately, with ethanol and heptane.

Alkanoic acids are known to chemisorb on the native oxide present on aluminum surfaces that have been exposed to air. Self-assembled monolayers of stearic acid ( $\text{CH}_3(\text{CH}_2)_{16}\text{COOH}$ ) were formed on aluminum surfaces in the following manner. 2000 Å of aluminum were vapor deposited on polished 4 in. diameter silicon wafers. The vapor deposition chamber was vented to pure oxygen so that the native oxide layer on the aluminum surface would not contain impurities from ambient room air. Immediately after removing the metal coated wafers from the vacuum chamber they were immersed in a 1mM solution of stearic acid in HPLC grade hexadecane. The hexadecane was eluted through an activity 1 alumina column prior to making the solution in order to remove impurities. The wafers were allowed to remain immersed in the solution for ~24 hrs whereupon they were removed and rinsed with HPLC grade heptane.

X-ray photoelectron spectroscopy studies of the resulting SAMs indicated that the aluminum layer was indeed coated with an organic film and that the film was stable at least to a temperature of 400% C. Contact angle measurements for the coated aluminum surfaces were 102% for water and 40% for hexadecane which are consistent with the presence of  $-\text{CH}_3$  groups at the air-monolayer interface.

We tested the corrosion inhibitive properties of the C18-monolayers by exposing the SAM-coated aluminum surfaces to sulfuric acid and then using Fourier transform infrared reflection absorption spectroscopy (FT-IRAS) to identify and quantify corrosion products [1].

Sulfuric acid is the principal corrosive agent in polluted urban and industrial atmospheres. Sub-micron thick films of sulfuric acid were formed on aluminum surfaces in vacuum by co-depositing  $\text{SO}_3$  and  $\text{H}_2\text{O}$ . Changes in the chemical composition of the sulfuric acid layer (including the appearance of  $\text{SO}_4^{2-}$ ,  $\text{H}_3\text{O}^+$ , and  $\text{HSO}_4^-$  and hydrated  $\text{Al}^{3+}$  ions) resulting from corrosion of the aluminum substrate, were monitored as a function of reagent concentration and relative humidity.

The FT-IRAS results indicate that, overall, the C18-monolayers do not significantly inhibit the sulfuric-acid induced corrosion of vapor-deposited Al surfaces. The corrosion products and their rate of appearance were essentially identical to those observed when no monolayer was present. This suggests that defects in the SAM allow the corrosive agents to fully penetrate the monolayer and react with the underlying aluminum substrate.

This conclusion was confirmed by experiments in which both SAM-coated and bare Al surfaces were exposed to a spray of 20 wt%  $\text{H}_2\text{SO}_4$ . Figure 1 shows photographs of these surfaces, which were allowed to remain at ambient humidity (~50%) for two days after spraying. The liquid acid droplets beaded up on the SAM-coated surface but spread uniformly on the bare Al surface. This is due to the C-18 SAM surface being hydrophobic and the native oxide covered Al surface being hydrophilic. On the Al surface, the acid reacts with the metal to form a layer of aluminum sulfate salt. The underlying dark Si substrate is visible. Underneath the acid droplets on the SAM-coated surface, dark spots are also visible, suggesting that the acid penetrates the

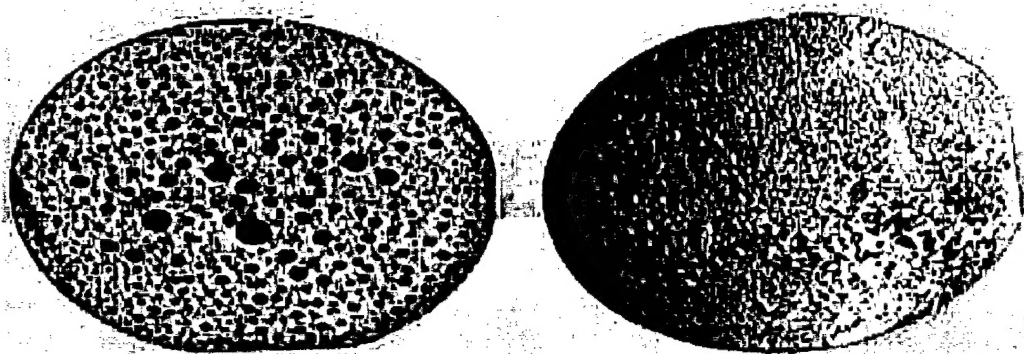


Figure 1 Photographs of C-18 SAM/Al/Si (left) and Al/Si (right) wafers 48 hrs after spraying with 20 wt% sulfuric acid solution. The dark spots on the left are due to beads of acid that form on the SAM surface and eventually penetrate the organic layer to corrode the underlying metal. The corrugated appearance of the wafer on the right is due to the formation of aluminum sulfate precipitate.

organic layer and corrodes the metal revealing the silicon wafer. X-ray photoelectron spectroscopy (XPS) measurements of the dark spots revealed exposed Si. Thus, the monolayer controls the wetting properties of the surface, but is not sufficiently thick to act as a barrier to corrosive agents. To the extent that the SAM coating limits the wettability of the surface by the acid, it also limits the degree of corrosion.

We also began to investigate the applicability of cross linked self-assembled films as corrosion protective coatings. Most organic primer coatings that are currently in use (e.g., epoxy resins) involve cross-linked systems of molecules. Cross-linking decreases the permeability of the film and increases its mechanical strength. We chose to study monolayers of 10,12-pentacosadiynoic acid [10,12-PDA;  $C_{25}H_{42}O_2$ ;  $CH_3(CH_2)_{11}C\equiv C-C\equiv C(CH_2)_8COOH$ ] since this compound has been observed to photopolymerize readily in Langmuir-Blodgett films under exposure to ultraviolet light [2-5]. Essentially,  $C\equiv C$  bonds rupture when irradiated leading to C-C bond formation across adjacent PDA chains. We expected that the carboxyl group at the end of the PDA chain would chemisorb onto the bare Al surface as it does with stearic acid.

The monolayer deposition experiments were performed in the following manner. Al-coated Si wafers were prepared as described above. They were then immersed in a ~1 mM solution of 10,12-PDA in HPLC grade hexadecane and allowed to remain in solution for ~24 hr. The wafers were then removed and rinsed thoroughly with hexadecane. All experiments were carried out under amber/red light to prevent photopolymerization. The wafers were stored in the dark.

Some of the wafers were then irradiated with ultraviolet light from a low pressure Hg lamp for 30 min in order to cross-link the triple bonds in adjacent 10,12-PDA molecules. The light flux on the wafers was ~10 mW/cm<sup>2</sup> and the radiation output peaks at 254 nm. The UV-irradiated and non-irradiated PDA-coated wafers were then subjected to different analytical tests. The corrosion resistance of the PDA-coated surfaces was tested using a spray of 20 wt%  $H_2SO_4$  as described above. Both the irradiated and non-irradiated PDA-coated surfaces displayed no corrosion inhibitive properties. The acid spread across the wafers and corroded both surfaces completely. XPS experiments indicated that the bare, uncoated Al surface had a large amount of adventitious carbon, presumably due to adsorption of atmospheric  $CO_2$  and hydrocarbons. The PDA-coated wafers (which were kept in vacuum prior to immersing in solution) had roughly the same carbon coverage as the uncoated Al wafers. Finally, polarization modulation FTIR experiments (performed by Dr. Larry Seger at the Army Research Laboratory) revealed identical

spectra for both the irradiated and non-irradiated PDA-coated surfaces. Dominant features included symmetric and asymmetric C-H stretching vibrations at  $\sim 3000\text{ cm}^{-1}$  [Figure 2]. No features due to C=C stretches were observed ( $\sim 2150\text{ cm}^{-1}$ ) [3] although these vibrations generally have very low absorption coefficients.

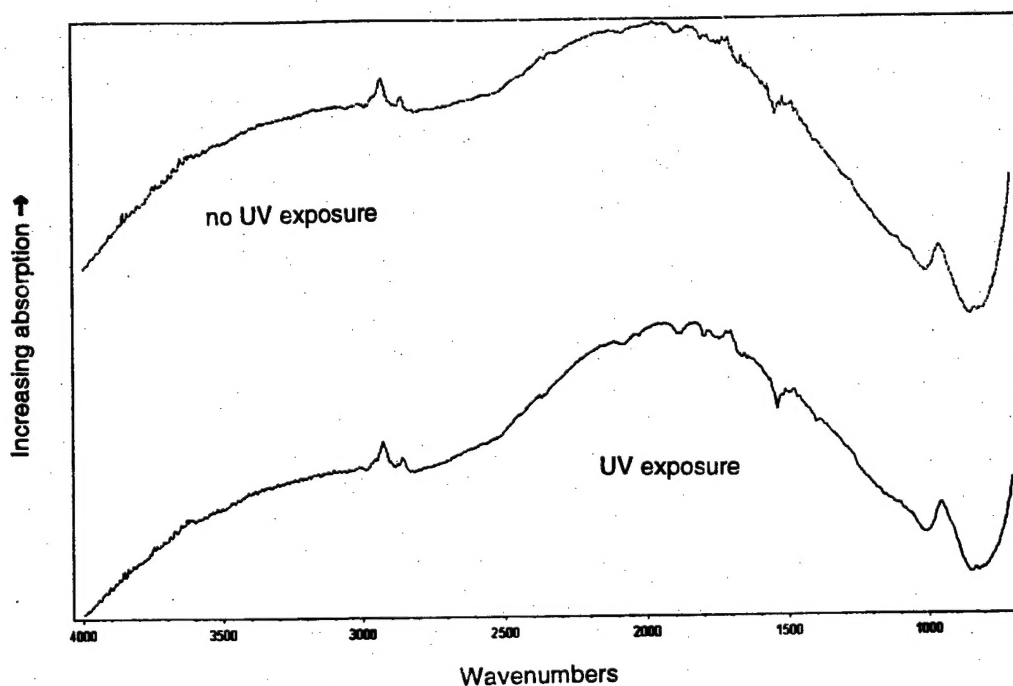


Figure 2. Polarization modulation infrared reflection absorption spectra of Al/Si wafers immersed in a 1 mM solution of 10,12-PDA and subsequently exposed to 10 mW of UV light for  $\sim 30$  min or not exposed (courtesy of Dr. Larry Seger, ARL).

Our results suggest either that 10,12-PDA has not chemisorbed on the native-oxide surfaces or that the PDA coverage is very low. In preparing the PDA/hexadecane solution, it was necessary to filter out what appeared to be insoluble, polymeric material. It is possible that the concentration of PDA is actually quite a bit lower than 1 mM. Alternatively, it is possible that the chemisorption probability of 10,12-PDA on native oxide-covered Al is much lower than that for stearic acid. Future experiments will involve variations in the procedure for forming PDA monolayers directed at enhancing the surface coverage.

As part of our overall effort to understand the physical properties of self-assembled monolayers, we spent some time during the past year finishing experiments and a paper on the surface potentials of fluorinated SAMs. Previous work in our laboratory on alkanethiolate SAMs [6] indicated that SAMs fluorinated using a beam of F atoms should be highly impermeable to gaseous reagents. In order to understand the electrical properties of such monolayers (and, by implication, their chemical properties), we have measured their static surface potentials. Our results [7] indicate that the electrical polarization of the beam-fluorinated monolayer is directly proportional to the degree of fluorination. In addition, the surface potentials displayed a small but finite temperature dependence. This result may have implications for the development of ultrathin film pyroelectric materials.

## REFERENCES

- 1) Q. Dai, A. Freedman, and G.N. Robinson, "Sulfuric Acid-Induced Corrosion of Aluminum Surfaces," *J. Electrochem. Soc.* **142**, 4063-4069 (1995).
- 2) N. Mino, H. Tamura, and K. Ogawa, "Analysis of Color Transitions and Changes on Langmuir-Blodgett Films of a Polydiacetylene Derivative," *Langmuir* **7**, 2336 (1991).
- 3) A. Saito, Y. Urai, and K. Itoh, "Infrared and Resonance Raman Spectroscopic Study on the Photopolymerization Process of the Langmuir-Blodgett Films of a Diacetylene Monocarboxylic Acid, 10,12-Pentacosadiynoic Acid," *Langmuir* **12**, 3938 (1996).
- 4) D.N. Batchelder, S.D. Evans, T.L. Freeman, L. Haussling, H. Ringsdorf, and H. Wolf, "Self-Assembled Monolayers Containing Polydiacetylenes," *J. Am. Chem. Soc.* **116**, 1050 (1994).
- 5) N. Mino, H. Tamura, and K. Ogawa, "Photoreactivity of 10,12-Pentacosadiynoic Acid Monolayers and Color Transitions of the Polymerized Monolayers on an Aqueous Subphase," *Langmuir* **8**, 594 (1992).
- 6) G.N. Robinson, A. Freedman, and R.L. Graham, "Reactions of Fluorine Atoms with Self-Assembled Monolayers of Alkanethiolates," *Langmuir* **11**, 2600 (1995).
- 7) G.N. Robinson, P.L. Kebabian, A. Freedman, and V. DePalma, "Temperature-Dependent Surface Potentials of Fluorinated Alkanethiolate Monolayers," *Thin Solid Films*, **310**, 24 (1997).

**TEMPERATURE-DEPENDENT SURFACE POTENTIALS OF  
FLUORINATED ALKANETHIOLATE SELF-ASSEMBLED  
MONOLAYERS**

by

Gary N. Robinson,\* Paul L. Kebabian, and Andrew Freedman  
Center for Chemical and Environmental Physics  
Aerodyne Research, Inc.  
45 Manning Road  
Billerica, MA 01821

and

Vito DePalma  
Eastman Kodak Company  
Rochester, NY 14650

Published in  
**Thin Solid Films** 310, 24 (1997)

## ABSTRACT

Self-assembled monolayers (SAMs) consisting of twenty-two carbon, methyl-terminated alkanethiolates adsorbed on vapor deposited gold have been fluorinated in vacuum using an effusive F atom source. The reactive uptake of fluorine as a function of F atom exposure was calibrated using X-ray photoelectron spectroscopy. The surface potentials ( $V_s$ ) of SAMs that were fluorinated to different degrees were measured as a function of temperature using a high-sensitivity vibrating probe electrostatic voltmeter. The surface potential grew increasingly negative with increasing fluorine uptake, reflecting the charge asymmetry that is induced in the alkanethiolate chains as a result of the substitution of fluorine for hydrogen. The  $V_s$  of the most highly fluorinated SAMs displayed a negative temperature dependence. This observation may be indicative of a pyroelectric effect in these monolayers although a definitive conclusion awaits further measurements.

## I. INTRODUCTION

Recent work in our laboratory has focused on modifying the surface properties of self-assembled monolayers (SAMs) composed of ordered, long-chain *n*-alkanethiolates adsorbed on gold ( $\text{CH}_3(\text{CH}_2)_n\text{S/Au}$ ) via fluorination of the carbon atoms near the air-monolayer interface [1]. In the present study, we have investigated the effect of such fluorination on the surface potentials of twenty-two carbon, methyl-terminated alkanethiolate SAMs. Our interest was primarily in determining what effect fluorination has on the temperature dependence of the monolayer's surface potential. Fluorination renders the chain molecules in the SAM dipolar. Since these molecules are highly oriented, fluorination should therefore create a permanent electrical polarization, or charge asymmetry, within the monolayer. To the extent that the orientation of the dipolar molecules within the fluorinated SAM is temperature dependent, the electrical polarization, and associated surface charge density and surface potential, of the monolayer should also vary with temperature. Such a variation in surface charge density with temperature is equivalent to pyroelectricity. Our approach to fluorinating the  $\text{CH}_3(\text{CH}_2)_{21}\text{S/Au}$  monolayers was to expose the SAMs to an effusive beam of fluorine atoms in vacuum. This technique allows us to introduce calibrated quantities of fluorine into the monolayer. Previous experiments indicated that the incoming F atoms penetrate the close-packed chains of the SAM and react to form mono- and difluorinated methylene groups [1]. Fluorination most likely occurs by incoming F atoms abstracting methylene hydrogen atoms on the chain, forming HF and creating radical sites for subsequent addition of F atoms. A maximum of seven out of twenty carbon atoms are fluorinated at room temperature, presumably because of steric crowding of the chains which prevents the F atoms from fully penetrating the layer.

---

In the present experiments,  $\text{CH}_3(\text{CH}_2)_{21}\text{S/Au}$  SAMs were fluorinated to different extents and the surface potentials of the resulting monolayers were measured as a function of temperature using a high-sensitivity vibrating microprobe electrostatic voltmeter. Surface potentials for the

fluorinated SAMs were measured relative to those of an unfluorinated reference monolayer. Our results indicate that fluorination significantly influences the surface potential of the twenty-two carbon chain monolayers. We have also observed a temperature dependence in the surface potentials of the fluorinated SAMs; however, attributing this observation unambiguously to a pyroelectric effect will require measurements of the electrical response of the fluorinated SAMs to a constant temperature ramp and/or to modulated infrared radiation [2-4]

## II. EXPERIMENTAL

### A. Sample Preparation

Self-assembled monolayer samples were made in the laboratory of Professor George M. Whitesides at Harvard University. The substrates were prepared by vapor depositing  $\sim 1000$  Å of gold onto 0.5 mm thick silicon (100) wafers pre-coated with  $\sim 10$  Å of titanium to promote adhesion. Self-assembled monolayers were formed by immersing the substrates overnight in a  $\sim 1$  mM solution of  $\text{HS}(\text{CH}_2)_{21}\text{CH}_3$ . Details of the synthesis procedures for these compounds are given in references 5-7. The samples were rinsed thoroughly with hexane and ethanol and blown dry with dry nitrogen prior to mounting in the vacuum chamber.

### B. Fluorination

The fluorination experiments were carried out in an ultrahigh vacuum apparatus consisting of a reaction chamber and a contiguous analysis chamber containing an X-ray photoelectron spectrometer. The reaction chamber is pumped by a turbomolecular pump and a liquid-nitrogen-cooled cryopanel. Atomic fluorine is produced in a microwave discharge plasma source consisting of a 1 cm diameter alumina flow tube surrounded by an Evenson-type microwave cavity [8]. A mixture of 5%  $\text{F}_2$  in argon at 2 Torr flows at a rate of  $\sim 150$  sccm through the tube. Running the discharge at 70 W produces 100% dissociation of the  $\text{F}_2$ . The output of the tube is sampled by a 40  $\mu\text{m}$  aperture resulting in an effusive F atom beam while the remainder of the gas flows through

a co-annular passage and is pumped by a mechanical pump. Assuming the F atom source to be effusive, we calculate a flux of  $\sim 9 \times 10^{13}$  atoms  $\text{cm}^{-2} \text{s}^{-1}$  at the sample surface. Possible errors in this calculation, including uncertainties in pressure, aperture size, and aperture-substrate distance are estimated to be  $\sim 25\%$ .

The samples were heated to  $\sim 335$  K under vacuum for about one hour prior to fluorinating. Fluorine dosing experiments were performed at a sample temperature of 305 K. The base pressure in the apparatus during these experiments was  $\sim 2 \times 10^{-9}$  Torr; the pressure in the reaction chamber with the beam on was  $\sim 1 \times 10^{-7}$  Torr.

### C. XPS Analysis

In order to determine the uptake of F atoms corresponding to a given F atom exposure, X-ray photoelectron spectroscopy (XPS) analysis experiments were performed. After exposure to a timed dose of F atoms, SAM samples were transferred using a linear motion manipulator to the ion-pumped analysis chamber. XPS analysis was performed using a PHI 15 keV Mg K $\alpha$  X-ray source at a photon energy of 1256.3 eV and a PHI double-pass cylindrical mirror energy analyzer operated at a bandpass energy of 25 eV. Spectra were recorded at each level of dosing for the C(1s), F(1s), and Au(4f) transitions. In addition, survey spectra were periodically recorded to check for contamination by water, oxygen, etc. The C(1s) and F(1s) intensities were normalized to the integrated Au(4f $_{7/2}$ ) signal in order to account for small changes in X-ray flux and the position of the surface in the spectrometer from run to run. The Au(4f $_{7/2}$ ) signal remained roughly constant during the experiments.

The XPS experiments were carried out in the first phase of our experimental study in order to calibrate the F atom uptake. No XPS measurements were performed on samples whose surface potentials were to be studied.

#### D. Surface Potential Measurements

Surface potentials ( $V_s$ ) of the SAMs were measured with a Trek Model 320B high-sensitivity, vibrating probe electrostatic voltmeter (Figure 1). The instrument is fitted with a custom-designed high-resolution miniature vibrating probe electrode (~1 mm diameter) for studying thin films and has been used to measure surface potentials of self-assembled monolayers [9,10]. A cylindrical brass shield surrounds the probe to minimize interference of stray electric fields with the voltage measurements. The temperature was controlled with a resistive heater and thermoelectric cooler that were attached to an aluminum block upon which the samples were clip-mounted. This block was attached to a positioning fixture with x, y, and z motion. A thermocouple was press fit against a reference sample to monitor the temperature. Electrical contact was made to the gold surface of the samples through the mounting clips. A small flow of dry nitrogen was introduced into the brass can during the measurements. The ambient relative humidity was ~50%.

Surface potentials were measured at temperatures in the range of 290-350 K for five samples that had been fluorinated to different degrees but *not* probed with XPS. An unfluorinated SAM served as a reference for the measurements. The  $V_s$  that are reported are therefore differences between the surface potentials of the fluorinated and unfluorinated monolayers. The precision of the measurements was  $\sim \pm 5$  mV.

### III. RESULTS

#### A. Calibration of Fluorine Uptake

X-ray photoelectron spectroscopy was used to calibrate the reactive uptake of fluorine atoms by monolayers of  $\text{CH}_3(\text{CH}_2)_{21}\text{S}/\text{Au}$ . The integrated intensities of the  $\text{F}(1s)$  spectra normalized to the integrated  $\text{Au}(4f_{7/2})$  XPS signal at 84.0 eV are plotted as a function of F atom exposure in Figure 2. X-ray exposure caused a small (<5%) amount of C-F bond breakage [1]. (Note that the surface potential measurements were performed on fluorinated SAMs that had not been exposed to X-rays.)

$\text{C}(1s)$  spectra were also recorded at each exposure. Since the resonance energy of fluorinated methylene (i.e.,  $-\text{CH}_2-$ ) carbon atoms is shifted relative to that of unsubstituted methylene carbon atoms, it was possible to determine the fraction of carbon atoms that were fluorinated at each exposure [1]. Knowing the coverage of the alkanethiolate chains in the monolayer ( $4.6 \times 10^{14} \text{ cm}^{-2}$ ), the number of carbon atoms per chain (22), and the fraction of fluorinated carbon atoms, it was then possible to determine the absolute number of F atoms bonded to the alkanethiolate chains. The ordinate-scale in Figure 2 is determined in this manner. Reference 1 gives a detailed description of this calculation and the uncertainties associated with it.

#### B. Surface Potential Measurements

The surface potential arises from the asymmetrical electric field that exists at the interface between two phases [11]. The net surface potential of a SAM of alkanethiolates on gold comprises contributions from the dipole moments of the Au-S bonds and of the alkane chains [9]. The net dipole moment of an unsubstituted alkanethiolate layer is directed towards the sulfur atoms since they draw electron density from the gold substrate. Fluorinating the chains will shift the net dipole

moment strongly in the opposite direction towards the surface of the monolayer [10].

The surface potential,  $V_s$ , of a SAM consisting of polar chains can be represented by the following equation (in SI units) [12],

Eq. 1

$$V_s = \frac{\sigma d}{D\epsilon_0}$$

where  $\sigma$  is the

surface charge density,  $d$  is the thickness of the monolayer,  $D$  is the relative dielectric constant of the monolayer, and  $\epsilon_0$  is the permittivity of free space. If the dielectric constant of the monolayer is known, measuring the surface potential will give the surface charge density directly and, when measured as a function of temperature, the charge density yields the pyroelectric coefficient,  $p$  (units of coulombs per  $m^2$  per Kelvin); thus,

Eq. 2.

$$p = \frac{\Delta\sigma}{\Delta T} = \frac{D\epsilon_0}{d} \frac{\Delta V_s}{\Delta T}$$

Surface potentials were measured as a function of temperature for five  $\text{CH}_3(\text{CH}_2)_{21}\text{S/Au}$  SAMs that underwent different amounts of beam-fluorination but were not probed with XPS. The fluorine exposures (40, 110, 210, 300, and  $610 \times 10^{15} \text{ cm}^{-2}$ ) are equivalent to five of the nine exposures plotted in Figure 2. (For convenience, we will refer to these five SAM samples by the numbers 1 - 5.) Values of  $V_s$  for these monolayers are plotted in Figure 3 as the difference between the surface potential of the fluorinated SAM and the surface potential of an unfluorinated reference SAM. The measurements on all five samples were carried out using the same reference monolayer.

The  $V_s$  display a distinct dependence on degree of fluorination, becoming more negative the more fluorinated the SAM. This reflects the charge asymmetry that is induced in the alkanethiolate chains as a result of the substitution of fluorine for hydrogen; the top of the monolayer is more negatively polarized than the bottom due to the presence of electronegative

fluorine atoms [10]. The thiolate-gold linkage should also become more polarized since the fluorinated chain can draw more electron density from the gold substrate.

Most striking is the pronounced temperature dependence of  $V_S$  for the three most highly fluorinated  $\text{CH}_3(\text{CH}_2)_{21}\text{S/Au}$  SAMs (Figure 3). As the SAMs are heated,  $V_S$  becomes increasingly negative suggesting that the net polarization of the monolayer increases with temperature. It is important to note that the measured  $V_S$  for the reference SAMs showed no temperature dependence.

Averaging the data for the three most highly fluorinated SAMs,  $\Delta V_S/\Delta T = -3.4 \pm 0.3$  mV/K. Measurements of monolayer 5 on a different day with a different reference monolayer yielded a higher absolute value of  $V_S$  (by  $\sim 0.1$  V) but the value of  $\Delta V_S/\Delta T$  was essentially unchanged.

#### IV. DISCUSSION

The chains in a methyl-terminated, alkanethiolate monolayer form an oriented, hexagonally close-packed monolayer [13] and, on Au, are canted roughly  $35^\circ$  from the surface normal [14,15]. Low-energy helium diffraction measurements on a monolayer of  $\text{CH}_3(\text{CH}_2)_n\text{SH}$  ( $n = 13, 16, 17, 21$ ) adsorbed on Au indicate that the lattice constant for the surface of the monolayer is  $5.01 \text{ \AA}$  [16] at 35 K. Most surface analytical and structural measurements indicate that these monolayers possess a high degree of surface order and uniformity.

---

Both He diffraction [16] and FTIR [17] measurements suggest, however, that the surfaces of  $\text{CH}_3$  terminated SAMs become disordered as the temperature of the monolayer is increased. Molecular dynamics studies by Klein and co-workers [18] indicate that the chain tilt angle (relative to the surface normal) decreases with increasing temperature. From Eq. 3, such a

decrease in tilt angle would cause the surface charge density,  $\sigma$  (and, from Eq. 1,  $V_S$ ) of the monolayer to increase. Thus,

$$\text{Eq. 3,} \quad \sigma = \frac{N\mu}{d} \cos\theta$$

(where  $N$  is the number of molecules per unit area,  $\mu$  is the dipole moment of the chains, and  $\theta$  is the angle between the molecular dipole moment and the surface normal) [12].

The change in surface potential with temperature that we observe for the three most fluorinated monolayers may indeed be due to such a collective change in tilt angle. Presumably monolayers 1 and 2 are insufficiently fluorinated to show a significant change in surface potential upon heating. This may be due to a smaller net polarization in these monolayers and/or to greater degree of order in the monolayer.

The beam-fluorinated monolayers will undoubtedly be somewhat disordered since the F atoms must penetrate the chains to abstract hydrogen and fluorinate the carbon atoms and F atoms are larger than H atoms [1]. For example, the chain-packing density of a SAM composed of (nearly) fully fluorinated chains is smaller than that of SAM composed of hydrogenated chains: the lattice constant of  $\text{CF}_3(\text{CF}_2)_{11}(\text{CH}_2)_2\text{S/Au}$  has been measured to be 5.7 Å [19] whereas the lattice constant of  $\text{CH}_3(\text{CH}_2)_{13}\text{S/Au}$  is 5.0 Å [16]. The increased disorder near the top of the beam-fluorinated SAMs would lessen the interchain van der Waals attractive forces present in a well-ordered monolayer, thereby enhancing the mobility of the chains and increasing the value of  $\Delta V_S/\Delta T$ . In monolayers 1 and 2, which are the least fluorinated and presumably the least disordered,  $\Delta V_S/\Delta T \approx 0$ .

If the observed change in surface potential with temperature is indicative of a change in the net polarization of the monolayer, it is possible to calculate pyroelectric coefficients for the fluorinated SAMs from  $\Delta V_s/\Delta T$  via Eq. 2. We assume  $D = 2.2$  (halfway between PTFE ( $D = 2.1$ ) and polyethylene ( $D = 2.3$ )). Ellipsometric measurements of  $\text{CH}_3(\text{CH}_2)_{21}\text{S/Au}$  SAMs yield a monolayer thickness of 29 Å [20]. Using our value of 3 mV/K for  $\Delta V_s/\Delta T$ , we calculate  $p = 2 \times 10^{-5} \text{ C m}^{-2} \text{ K}^{-1}$  or  $20 \mu\text{C m}^{-2} \text{ K}^{-1}$  for the three most highly fluorinated monolayers. This value of  $p$  is comparable in magnitude to those for polymer pyroelectrics. At 300 K, polyvinylidene fluoride (PVDF) has a pyroelectric coefficient of 30 - 45  $\mu\text{C m}^{-2} \text{ K}^{-1}$  [21-23] and the co-polymer polyvinylidene fluoride-trifluoroethylene has a coefficient of 40 - 50  $\mu\text{C m}^{-2} \text{ K}^{-1}$ . [24]. Noncentrosymmetric, multilayer Langmuir-Blodgett (LB) films have been created which have values of  $p$  between 0.2 - 2  $\mu\text{C m}^{-2} \text{ K}^{-1}$  [4, 25-29]. However, there has been a report of a pyroelectric coefficient of 22  $\mu\text{C m}^{-2} \text{ K}^{-1}$  for an LB film composed of azobenzene-derivatized alkane chains [30].

Ascribing our observation of a temperature-dependent  $V_s$  for the fluorinated monolayers to a pyroelectric effect is rather tentative at this point. Our experimental method differs from the commonly used static and dynamic methods for measuring pyroelectric coefficients [2-4], which require electrical contacts on both sides of the material being studied. In the static method, a linear temperature ramp is applied to the material and the resulting current is measured with an electrometer. In the dynamic method, a lock-in amplifier is used to measure the electrical response of the material to modulated infrared radiation. Such measurements would be challenging on a SAM since it would not be easy to make electrical contact with the top of the monolayer without shorting through the layer. Nonetheless, in order to determine definitively the source of the observed temperature dependence in our beam-fluorinated SAMs, it will be necessary to place an electrode on top of the monolayer and to carry out one or both of the pyroelectric measurements commonly employed.

## ACKNOWLEDGMENTS

This work was supported by the National Science Foundation through the Small Business Innovation Research program and by the U.S. Army Research Office (Contract No. DAAH04-95-C-0012). We are grateful to Hans Biebuyck, Rebecca Jackman, and Prof. George Whitesides for providing the monolayer samples.

## REFERENCES

1. G.N. Robinson, A. Freedman, and R.L. Graham, *Langmuir* **11**, 2600 (1995).
2. R.L. Byer and C.B. Roundy, *Ferroelectrics* **3**, 333 (1972).
3. A.G. Chynoweth, *J. Appl. Phys.* **27**, 78 (1956)
4. G.W. Smith, M.F. Daniel, J.W. Barton, and N. Ratcliffe, *Thin Solid Films* **132**, 125 (1985).
5. C.D. Bain, E.B. Troughton, Y-T. Tao, J. Evall, G.M. Whitesides, and R.G. Nuzzo, *J. Am. Chem. Soc.* **111**, 321 (1989).
6. P.E. Laibinis and G.M. Whitesides, *J. Am. Chem. Soc.* **114**, 9022 (1992).
7. R.L. Graham, C.D. Bain, H.A. Biebuyck, P.E. Laibinis, and G.M. Whitesides, *J. Phys. Chem.* **97**, 9456 (1993).
8. C.D. Stinespring, A. Freedman, and C.E. Kolb, *J. Vac. Sci. Technol.* **A4**, 1946 (1986).
9. S.D. Evans and A. Ulman, *Chem. Phys. Lett.* **170**, 462 (1990).
10. S.D. Evans, E. Urankar, A. Ulman, and N. Ferris, *J. Am. Chem. Soc.* **113**, 4121 (1991).
11. G.L. Gaines, Jr., *Insoluble Monolayers at Liquid-Gas Interfaces*, (John Wiley, 1966).
12. A. Ulman, *An Introduction to Ultrathin Organic Films: from Langmuir-Blodgett to Self-Assembly* (Academic Press, 1991), Chapter 1.
13. L. Strong and G.M. Whitesides, *Langmuir* **4**, 546 (1988).
14. R.G. Nuzzo, L.H. Dubois, and D.L. Allara, *J. Am. Chem. Soc.* **112**, 558 (1990).
15. L.H. Dubois, B.R. Zegarski, and R.G. Nuzzo, *Proc. Nat'l. Acad. Sci.* **84**, 4739 (1987).
16. N. Camillone III, C.E.D. Chidsey, G.-Y. Liu, T.M. Putvinski, and G. Scoles, *J. Chem. Phys.* **94**, 8493 (1991).
17. R.G. Nuzzo, E.M. Korenic, and L.H. Dubois, *J. Chem. Phys.* **93**, 767 (1990).
18. J. Hautman and M.L. Klein, *J. Chem. Phys.* **93**, 7483 (1990); J. Hautman and M.L. Klein, *J. Chem. Phys.* **91**, 4994 (1989).
19. G.-Y. Liu, P. Fenter, C.E.D. Chidsey, D.F. Ogletree, P. Eisenberger, and M. Salmeron, *J. Chem. Phys.* **101**, 4301 (1994).
20. J.P. Folkers, P.E. Laibinis, and G.M. Whitesides, *Langmuir* **8**, 1330 (1992).
21. R.W. Whatmore, *Rep. Prog. Phys.* **49**, 1335 (1986).
22. H. Sussner, D.E. Horne, and D.Y. Yoon, *Appl. Phys. Lett.* **32**, 137 (1978).
23. G.M. Sessler, *J. Acoust. Soc. Am.* **70**, 1596 (1981).
24. N. Neumann, R. Köhler, and G. Hoffman, *Ferroelectrics* **118**, 319 (1991).

25. C.A. Jones, M.C. Petty, and G.G. Roberts, Thin Solid Films 160, 117 (1988).
26. G.W. Smith, N. Ratcliffe, S.J. Roser, and M.F. Daniel, Thin Solid Films 151, 9 (1987).
27. G. Roberts and B. Holcroft, Thin Solid Films 180, 211 (1989).
28. G.W. Smith and T.J. Evans Thin Solid Films 146, 7 (1987).
29. P. Christie, G.G. Roberts, and M.C. Petty, Appl. Phys. Lett. 48, 1101 (1986).
30. J. Yang, R. Wang, D. Tang, L. Jiang, and T. Li, Chem. Phys. Lett. 197, 369 (1992).

## FIGURE CAPTIONS

- Figure 1. Schematic of vibrating probe electrostatic voltmeter apparatus used for surface potential measurements on twenty-two carbon alkanethiolate SAMs on gold-coated Si.
- Figure 2. F atom uptake by  $\text{CH}_3(\text{CH}_2)_{21}\text{S/Au}$  as a function of exposure. Circles represent integrated F(1s) X-ray photoelectron spectra. The procedure for determining the ordinate scale is given in Reference 1.
- Figure 3. Surface potentials as a function of temperature for five  $\text{CH}_3(\text{CH}_2)_{21}\text{S/Au}$  SAM samples fluorinated to different degrees. The sample numbers referred to in the text are noted next to the F atom exposures.

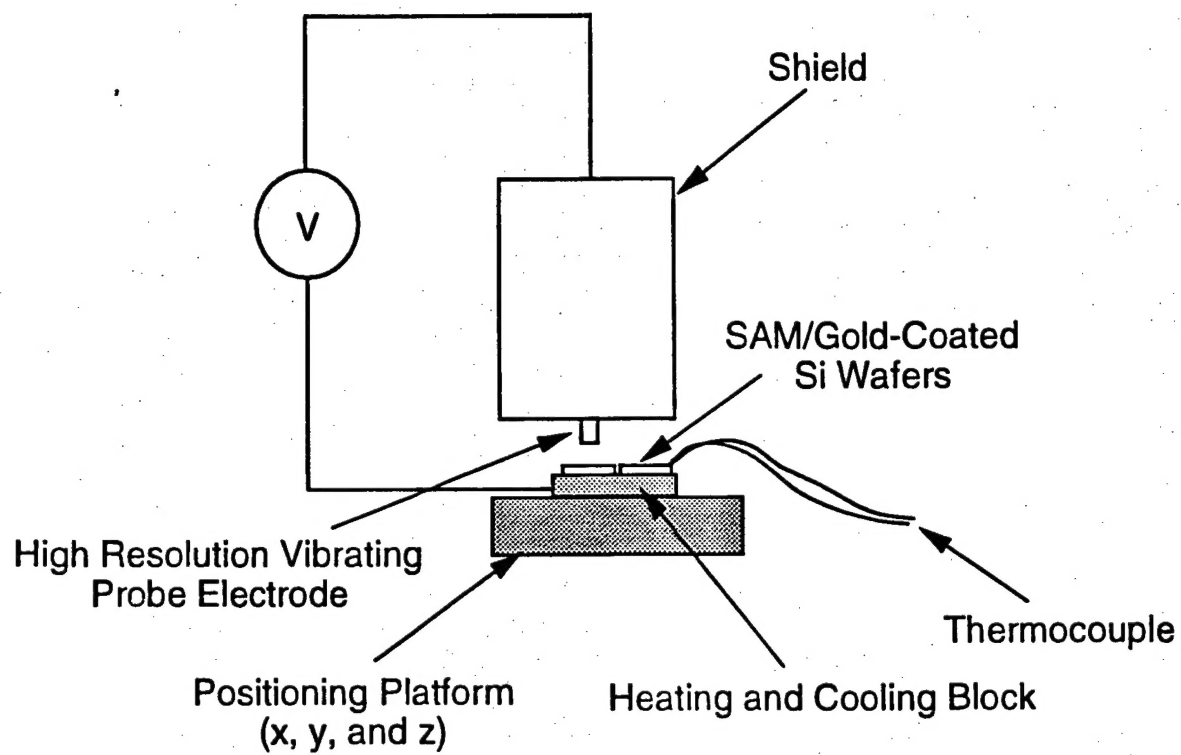


Figure 1

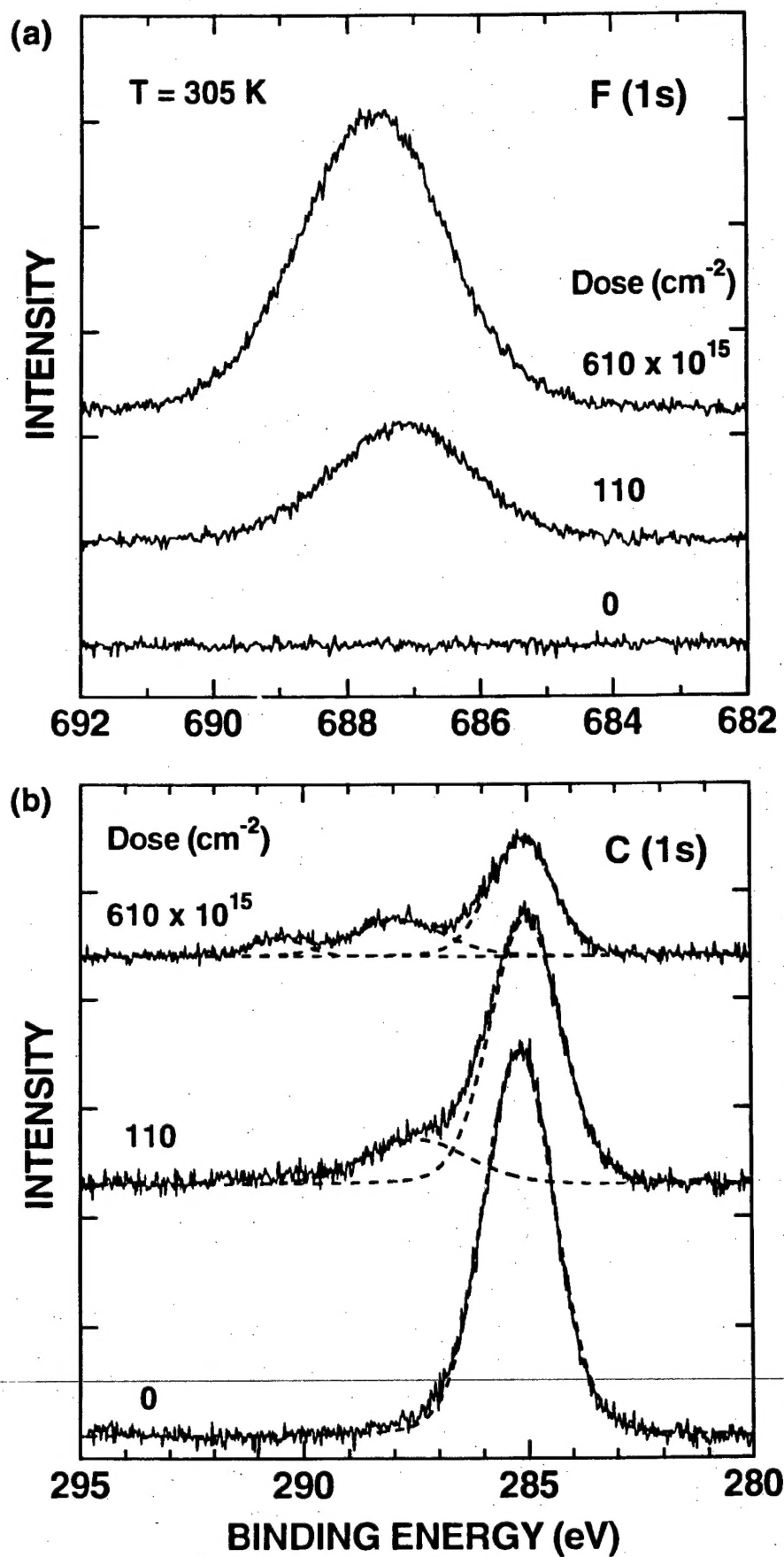


Figure 2

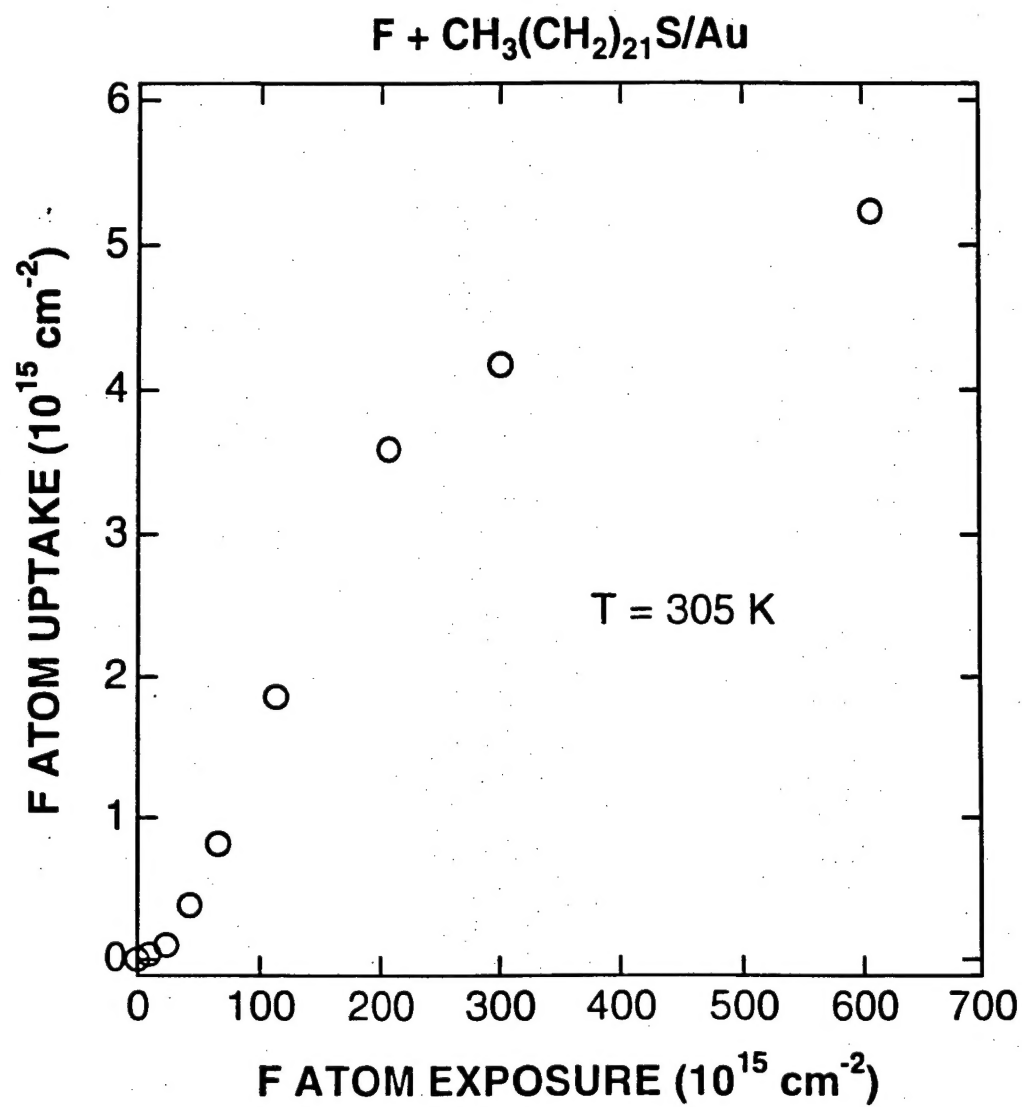


Figure 3

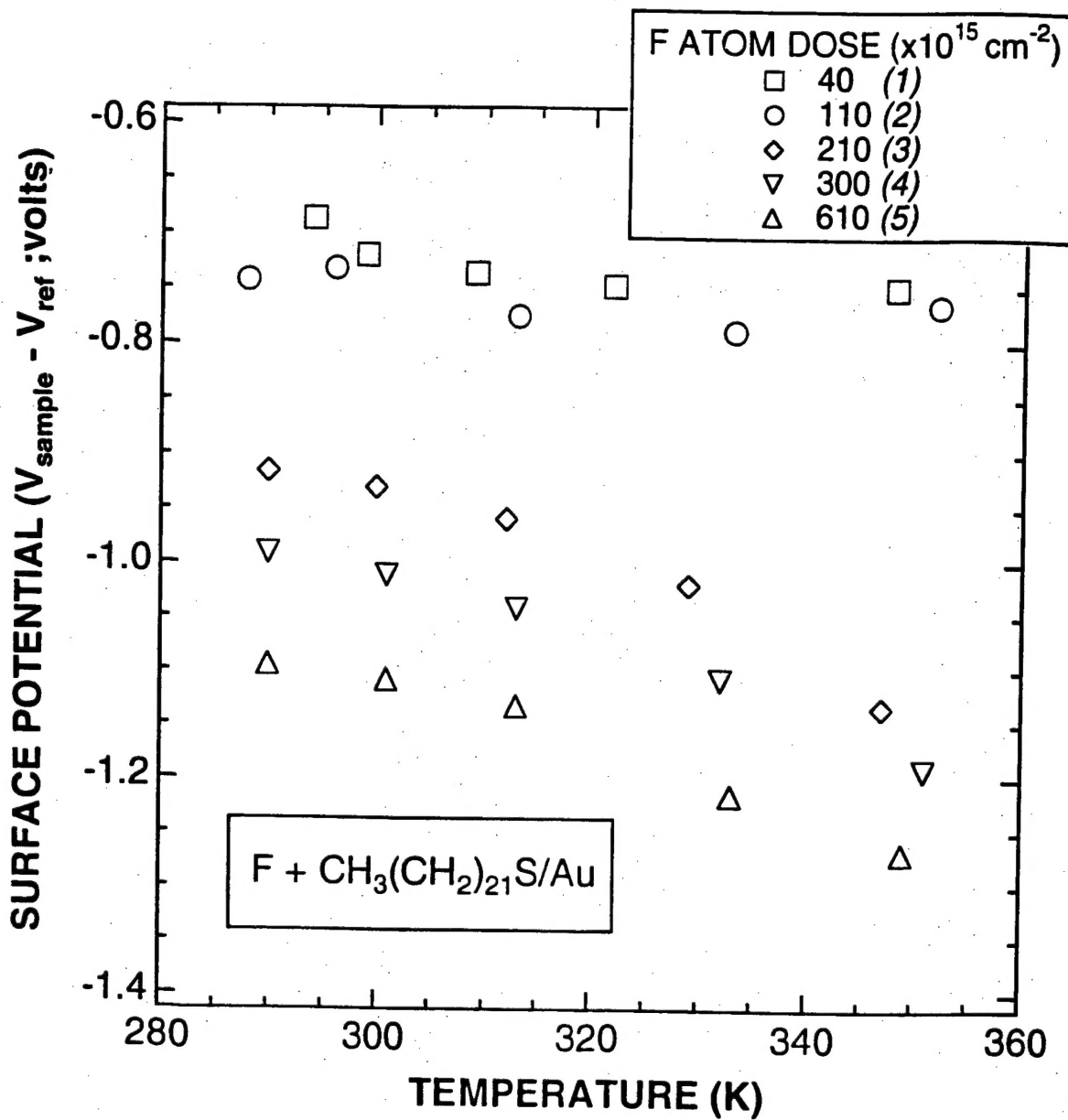


Figure 34